Polarized single crystal neutron diffraction study of the zero-magnetization ferromagnet Sm$_{1-x}$Gd$_x$Al$_2$ ($x = 0.024$)

T. Chatterji,[*] A. Stunault, and P. J. Brown

Institut Laue-Langevin, 71 Avenue des Martyrs, 38000 Grenoble, France

We have determined the temperature evolution of the spin and orbital moments in the zero-magnetization ferromagnet Sm$_{1-x}$Gd$_x$Al$_2$ ($x = 0.024$) by combining polarized and unpolarized single crystal neutron diffraction data. The sensitivity of the polarized neutron technique has allowed the moment values to be determined with a precision of $\approx 0.1\mu_B$. Our results clearly demonstrate that, when magnetized by a field of 8 T, the spin and orbital moments in Sm$_{1-x}$Gd$_x$Al$_2$ are oppositely directed, so that the net magnetization is very small. Below 60 K the contributions from spin and orbital motions are both about $2\mu_B$, with that due to orbital motion being slightly larger than that due to spin. Between 60 and 65 K the contributions of each to the magnetization fall rapidly and change sign at $T_{\rm comp} \approx 67$ K, above which the aligned moments recover but with the orbital magnetization still slightly higher than the spin one. These results imply that above $T_{\rm comp}$ the small resultant magnetization of the Sm^{3+} ion is oppositely directed to the magnetizing field. It is suggested that this anomaly is due to polarization of conduction electron spin associated with the doping Gd^{3+} ions.

I. INTRODUCTION

Strong spin-orbit interaction [1–3] is known to lead to interesting physics in, for example, topological insulators [4–6], thermoelectric materials [7–11], Dzyaloshinskii-Moriya weak ferromagnets [12], etc. Among these the rare-earth ion Sm^{3+} presents a unique case since the ion has spin and orbital magnetic moments, both about $4\mu_B$, which are strongly coupled antiparallel to one another so that they almost cancel out. In most rare-earth elements, the ground J multiplet is sufficiently separated from other multiplets that both the spin and orbital moments can be expressed in terms of the same operator of the total angular momentum. This implies that they have the same temperature dependence. However, for Sm^{3+} a few low-level multiplets with different J values lie close enough in energy to the ground multiplet to mix with it. Due to this mixing the spin and orbital moments in Sm^{3+} depend upon distinct operators. The degree of admixture of close multiplets and its temperature variation in the solid may lead to exact cancellation of the spin and orbital moments in a narrow range of temperature, giving rise to the so-called zero-magnetization ferromagnet (ZMF). Studies of the temperature dependence of magnetization in SmAl$_2$ suggest that in the pure compound the admixture of multiplets is not enough to cause complete cancellation; however, doping SmAl$_2$ with Gd^{3+}, which has a large spin-only moment, does lead to a zero-magnetization ferromagnet, Sm$_{2-x}$Gd$_x$Al$_2$ [13]. For $x = 0.0185$ the compensation temperature $T_{\rm comp} \approx 80$ K, with a ferromagnetic transition temperature $T_C \approx 120$ K.

The unique properties of zero-magnetization ferromagnets are well suited for use in devices processing the spin of charged particles. ZMF materials, despite their uniform spin polarization, do not generate stray magnetic fields which perturb the motion of charged particles and so can be used in spin electronics manipulating both electric current and spin polarization.

The behavior with varying temperature of the oppositely oriented spin and orbital moments of Sm^{3+} in a solid-state environment has been studied in the zero-magnetization ferromagnet Sm$_{1-x}$Gd$_x$Al$_2$, $x = 0.18$, using several different techniques [14–17]. It is not easy to determine the orbital and spin moments separately. Neutron diffraction cannot separate these moments directly, but they do have distinct cross sections for scattering of elliptically polarized x rays. Results, using this technique, show a distinct crossover of spin and orbital moments at $T_{\rm comp} \approx 80$ K [15]. Qiao *et al.* [16] used x-ray magnetic circular dichroism to determine the temperature dependence of the spin and orbital contributions to the moments of the Sm and Gd ions separately. They concluded that conduction electrons contribute almost as much to the magnetization as the spin of Sm^{3+} with the same temperature variation. Complementing these studies of spin and orbital moments, helicity switching Compton scattering [14] and specific-heat measurements [15] have been used to prove that ferromagnetic order persists through the whole of the compensation region. Muon spin rotation investigations [17] have also been carried out on these ZMF Sm$_{1-x}$Gd$_x$Al$_2$ materials. Gotsis and Mazin [18] calculated the electronic structure and magnetic properties of ferromagnetic SmAl$_2$ using the local-spin-density approximation (LSDA) $+ U$, and they found that this method can give a physically meaningful description of spin-orbit compensation in Gd-doped SmAl$_2$.

Although, as noted above, neutron diffraction cannot separate the spin and orbital contributions to the magnetic moments directly, the cross section for magnetic neutron scattering by the Sm^{3+} ion can be modeled in terms of these two parameters using the dipole approximation [19]. In this approximation the
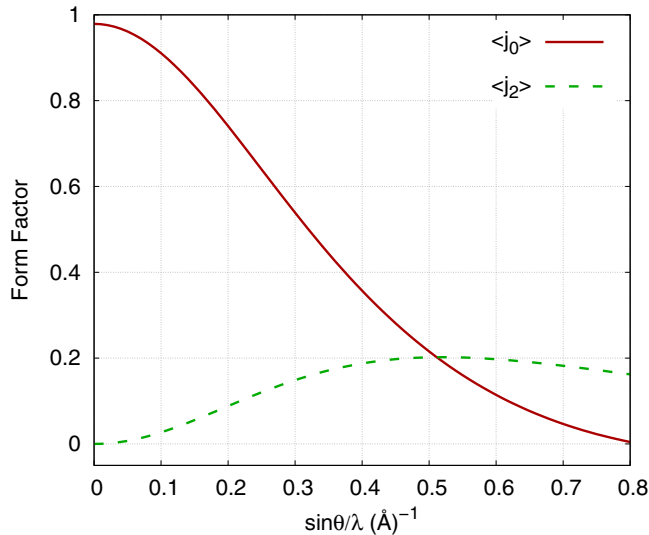
FIG. 1. Form factors [20] $\langle j_0 \rangle$ and $\langle j_2 \rangle$ for Sm^{3+}.

amplitude of magnetic scattering by the ion may be expressed as a function of the scattering vector k as

$$f(k) = \langle j_0(k) \rangle \hat{\mathbf{S}} + [\langle j_0(k) \rangle + \langle j_2(k) \rangle] \hat{\mathbf{L}}. \quad (1)$$

Here $\hat{\mathbf{S}}$ and $\hat{\mathbf{L}}$ are the mean spin and orbital quantum numbers for the ion, and the form factors $\langle j_l(k) \rangle$ are calculated from the radial distribution $U^2(r)$ of the $4f$ electrons in the ion using

$$\langle j_l(k) \rangle = \int U^2(r) j_l(kr) 4\pi r^2 \, dr, \quad (2)$$

in which $j_l(kr)$ are spherical Bessel functions. The variation with $k \propto \sin\theta/\lambda$ of $\langle j_0 \rangle$ and $\langle j_2 \rangle$ for Sm^{3+} is shown in Fig. 1, from which it can be seen that they vary very differently between $k = 0$ and 0.8 Å^{-1}. We have exploited this difference to determine the temperature variations of the spin and orbital contributions to the magnetic moment of Sm^{3+} in $Sm_{0.976}Gd_{0.024}Al_2$ separately. Although the total magnetization of the ZMF $Sm_{0.976}Gd_{0.024}Al_2$ is rather small, these separate components can be determined with high precision using polarized neutron diffraction because the polarized neutron intensity asymmetry depends on the ratio between the magnetic and nuclear structure factors rather than on the sum of their squares, as is the case for unpolarized neutrons. To determine magnetic form factors from polarized neutron asymmetries, the nuclear structure factors must be known to the required precision, and in particular, extinction effects, which invalidate the proportionality between the scattered intensity and the square of the structure factor, must be modeled accurately.

Neutron diffraction studies of Gd and Sm compounds are difficult because of the high absorption cross sections of both these elements for thermal neutrons ($> 10^4$ barns) [21]. This difficulty can be greatly reduced by using "hot" neutrons available from the Institut Laue-Langevin (ILL) hot source. With neutron energies of ≈ 300 mev ($\lambda = 0.5$ Å) the absorption cross section is reduced by a factor of about 40, leading to a linear absorption coefficient less than 1 mm^{-1} for SmAl$_2$. The polarized and unpolarized neutron diffraction measurements described here were made possible by using these shorter

wavelengths. SmAl$_2$ has the C14 cubic Laves phase structure, space group $Fd3m$. Both the Sm and Al atoms occupy special positions: Sm occupies 8a ($\frac{1}{8}, \frac{1}{8}, \frac{1}{8}$), and Al occupies 16d ($\frac{1}{2}$, $\frac{1}{2}, \frac{1}{2}$). The only free parameters affecting the nuclear structure factors are the scattering length of the rare-earth site (SmGd), which is not accurately known at short wavelengths, and the Sm and Al isotropic temperature factors. It may be noted that at these short wavelengths the contribution to the scattering cross sections of the imaginary part of the rare-earth scattering length (≈ 0.2 fm) can be neglected.

II. EXPERIMENT

Single crystals of $Sm_{.976}Gd_{.024}Al_2$ were grown from the melt using both the Bridgeman and Czochralski methods. Neutron diffraction measurements were made on two crystals of nominal composition, $Sm_{0.976}Gd_{0.024}Al_2$, and approximate volumes of 500 mm^3 (crystal X1) and 20 mm^3 (crystal X2). Magnetization measurements [14] confirmed their ZMF properties.

A. Unpolarized neutron intensity measurements

Integrated intensity measurements were made on the four-circle hot source diffractometer D9 at the Institut Laue-Langevin in Grenoble. The sample temperature was controlled by a two-stage displex refrigerator. The integrated intensities of all accessible reflections with $\sin\theta/\lambda < 0.85$ Å^{-1} were measured from X1 at temperatures of 30, 62, and 100 K using a neutron wavelength of 0.51 Å. The cubic symmetry allowed many equivalents of each of the independent reflections to be measured. These showed a spread in intensity of up to a factor of 2 which was attributed to the variations in absorption due to the asymmetric shape of the crystal. Intensities measured up to $\sin\theta/\lambda = 0.5$ Å^{-1} from the much smaller crystal, X2, at 70 K showed, as expected, much less divergence between equivalent reflections.

B. Polarized neutron intensity asymmetry

Polarized neutron measurements were made using the spin-polarized diffractometer D3 at ILL, which also receives neutrons from the hot source. The crystals were mounted in an asymmetric split-pair cryomagnet and magnetized with a vertical field of 8T. The asymmetry in the peak intensities of Bragg reflections for 0.52-Å neutrons polarized parallel and antiparallel to the field direction were made on both crystals at temperatures in the range 32–105 K. With the large crystal, X1, a significant asymmetry was measured in 24 independent reflections with $0.21 < \sin\theta/\lambda < 1.14$ Å^{-1}, whereas for the small crystal, X2, only 12 independent reflections with $0.21 < \sin\theta/\lambda < 0.72$ Å^{-1} could be measured.

III. RESULTS

A. Nuclear structure model

A linear absorption coefficient $\mu = 0.38$ mm^{-1} for $\lambda = 0.51$ Å was estimated from the curve of total cross section vs energy given by Lynn and Seeger [21]. Transmission factors for all measured reflections were calculated using this
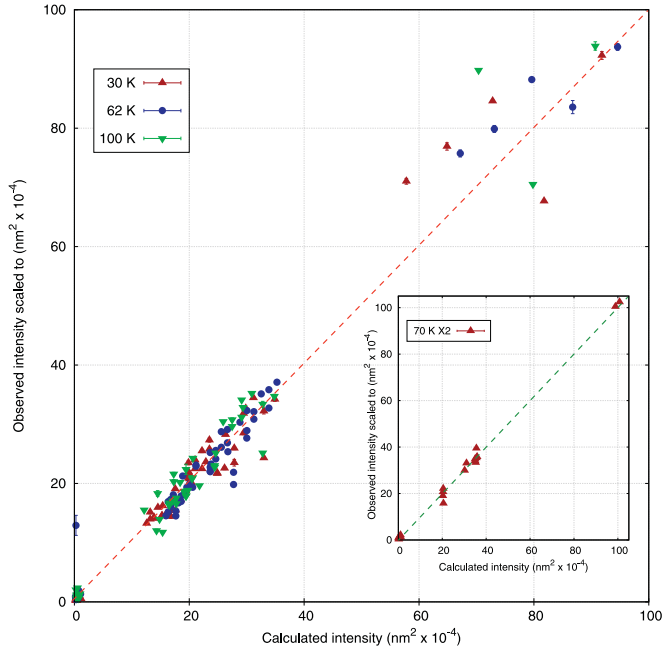
FIG. 2. The squares of the structure factors measured for crystal X1 at three temperatures plotted against their values calculated from model B. The inset shows the same plot for reflections measured from the smaller crystal, X2.

coefficient and approximate models of the crystal shapes. Applying this correction led to a marked reduction in the spread of intensities for the symmetry-related reflections from crystal X1. The transmission factors calculated for this crystal varied between 0.04 and 0.184, whereas for crystal X2 the range was only 0.50 to 0.53.

After correcting for absorption, the mean structure amplitude was calculated for each independent reflection in the sets measured at each temperature. These structure amplitudes were used as data in least-squares refinements in which, initially, the free parameters were a scale factor, the Sm site scattering length b_{Re}, the Sm and Al isotropic temperature factors B_{Re} and B_{Al}, and a single extinction parameter (mosaic spread). These initial refinements led to unphysical (negative)

TABLE I. Results obtained from least-squares refinements of the nuclear structure parameters of $Sm_{0.976}Gd_{0.024}Al_2$.

T	Crystal	b_{Re} (fm)	B_{Re} (Å^{-2})	B_{Al} (Å^{-2})	Scale	N_{obs}	R_{cryst}[a](%)
			(a) All parameters varied				
30	X1	5.9(3)	0.42(11)	0.69(9)	19.7(6)	55	7.1
62	X1	6.0(1)	0.29(5)	0.44(6)	19.6(5)	72	6.3
100	X1	5.2(2)	0.19(6)	0.51(6)	19.4(3)	70	5.3
70	X2	5.2(3)	−0.2(2)	0.3(2)	2.31(8)	20	4.5
		(b) b_{Re} = 5.65(23) fm; scale for X1 = 19.5(4)					
30	X1		0.28(5)	0.69(5)			7.1
62	X1		0.20(3)	0.45(3)			5.9
100	X1		0.38(3)	0.52(3)			5.5
70	X2		0.03(20)	0.11(18)			4.4

[a]$R_{cryst} = (\sum_1^{N_{obs}} |F_{obs} - F_{calc}|)/(\sum_1^{N_{obs}} |F_{obs}|)$, where F_{obs} and F_{calc} are the absolute values of the observed and calculated structure factors and N_{obs} is the number of observations.

values for the mosaic spread parameter, suggesting that the degree of extinction was small. They also indicated a high degree of correlation between the isotropic temperature factors and the other parameters. Further refinements were carried out without extinction, giving the results shown in Table I(a). To reduce the effects of correlation in further refinements the Sm scattering length was fixed to the value 5.65 fm obtained from the weighted mean of its four values in Table I(a), and the scale for all X1 data was fixed to the mean of the three values obtained with b_{Re} fixed. The final results for which only the temperature factors were refined are in Table I(b). Since the amplitudes of thermal vibrations are not expected to vary much in this temperature range and the differences in the refined B values are hardly significant, the mean values $B_{Re} = 0.29(5)$ and $B_{Al} = 0.51(5)$ were used at all temperatures in subsequent calculations.

Figure 2 shows the squares of the experimental structure factors plotted against the corresponding values calculated for model structure B. It can be seen that there is a good linear dependence between the two. The scatter in the high-intensity reflections from crystal X1 is probably due to inadequacy in the absorption corrections due to difficulty in accurately describing the crystal shape. Most importantly, the good linearity confirms the absence of any significant extinction, allowing the polarized neutron intensities to be analyzed using a zero-extinction model.

B. Spin and orbital moments from polarized neutron asymmetry

The polarized neutron intensity asymmetry for a magnetized ferromagnet is defined as $A = (I^+ - I^-)/(I^+ + I^-)$,

TABLE II. Parameters obtained by fitting Eq. (8) to the aligned magnetic moment $\mu_0 f(k)$ of Sm in $Sm_{0.976}Gd_{0.024}Al_2$ measured at temperatures T.

| T (K)	a_{j0}	a_{j2}	μ_0 (units of μ_B)	N_{obs}
		Crystal X1		
32.86	−2.57(9)	2.78(8)	0.22(2)	15
56.48	−2.17(13)	2.29(13)	0.120(12)	3
58.32	−2.21(13)	2.34(13)	0.13(2)	4
59.60	−2.0(4)	2.1(4)	0.07(13)	4
60.68	−0.58(6)	0.68(6)	0.10(2)	17
62.51	−0.06(4)	0.11(4)	0.049(8)	13
65.33	−0.04(7)	0.08(7)	0.041(7)	4
68.92	0.44(6)	−0.42(6)	0.025(12)	4
70.08	1.2(2)	−1.3(2)	−0.02(2)	3
71.45	1.72(6)	−1.79(6)	−0.068(10)	15
104.08	1.1(2)	−1.2(2)	−0.04(2)	14
		Crystal X2		
32.95	−1.70(6)	1.93(6)	0.235(8)	12
49.17	−1.8(3)	2.0(3)	0.18(3)	6
58.92	−1.44(7)	1.62(7)	0.179(10)	6
62.93	−1.49(6)	1.64(6)	0.149(6)	6
64.80	−1.41(5)	1.56(5)	0.149(5)	6
67.03	−0.40(14)	0.37(14)	−0.02(4)	12
68.68	1.32(11)	−1.37(11)	−0.044(13)	8
69.70	1.41(12)	−1.47(12)	−0.056(14)	8
73.44	1.34(5)	−1.40(5)	−0.059(7)	12
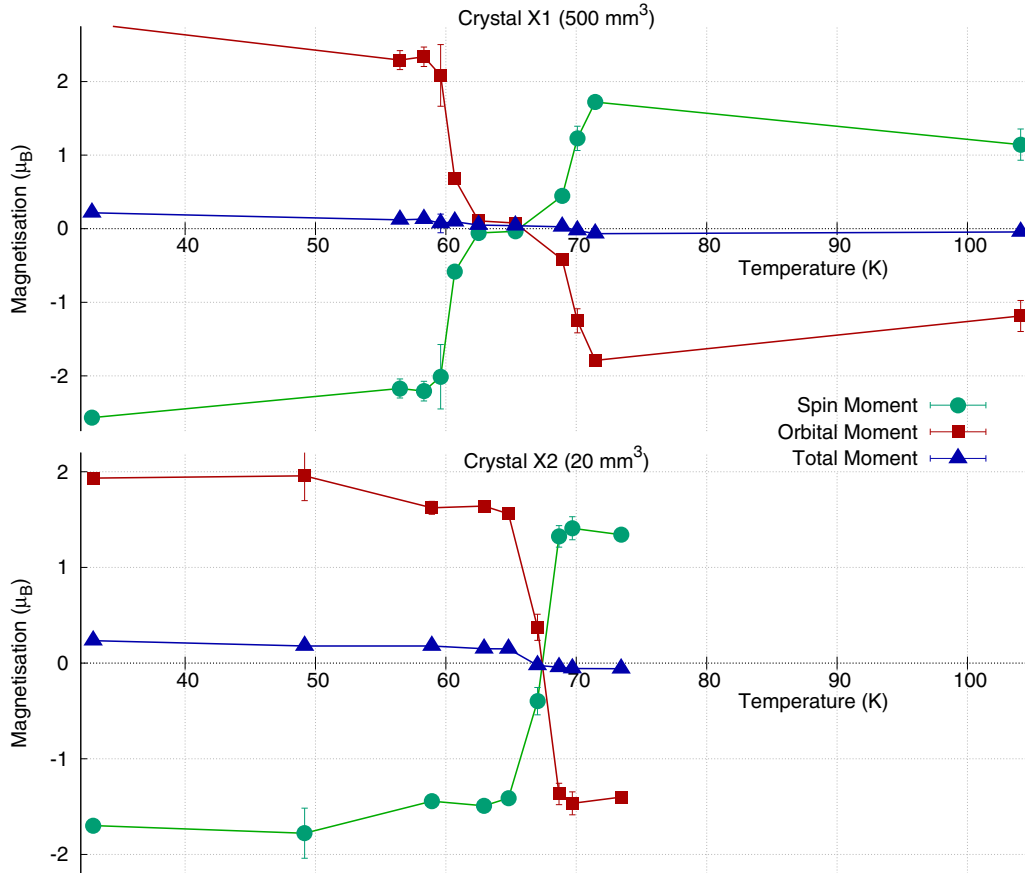
FIG. 3. Variation with temperature of the spin and orbital contributions to the magnetization aligned by a field of 8 T in $Sm_{0.976}Gd_{0.024}Al_2$.

where I^+ and I^- are the intensities measured with neutrons polarized parallel and antiparallel to the magnetizing field. In the absence of extinction the asymmetry measured with polarizing efficiency P for a reflection with the scattering vector inclined at an angle $90 - \rho$ to the field is given in terms of the magnetic and nuclear structure factors F_M and F_N by

$$A = \frac{2P F_N F_M \cos^2 \rho}{F_N^2 + F_M^2 q^4} = \frac{Pq\gamma}{1 + q^2\gamma^2},$$
$$q = \cos^2 \rho, \qquad \gamma = F_M/F_N. \qquad (3)$$

The polarizing efficiency P determined for D3 with $\lambda = 0.53$ Å, $H = 8$ T is 0.95(1).

Equation (3) was used to calculate the ratio γ for all the asymmetries measured in the experiment, and these were than used to determine the temperature variation of the aligned magnetization and its form factor. The magnetic structure factor for $SmAl_2$ depends just on the rare-earth ion,

$$F_M(k) = \mu_0 f(k) G_{Re} T_{Re}, \qquad (4)$$

where μ_0 is the Sm magnetic moment, $f(k)$ is its magnetic form factor, G_{Re} is its geometric structure factor, and T_{Re} is the factor $[\exp -(B_{Re}k^2)]$ by which thermal vibrations reduce the structure amplitude. The nuclear structure factor, on the other hand, depends on both Sm and Al:

$$F_N(k) = b_{Re} G_{Re} T_{Re} + b_{Al} G_{Al} T_{Al}, \qquad (5)$$

$$\mu_0 f(k) = \gamma \left(b_{Re} + b_{Al} \frac{G_{Al} T_{Al}}{G_{Re} T_{Re}} \right) = \gamma (b_{Re} + b_{Al} R). \qquad (6)$$

Since the purpose of the experiment is to determine the magnetic form factor for Sm, one must consider to what extent uncertainties in the parameters of the model may affect the result. For $SmAl_2$ these are in just b_{Re} and the ratio T_{Al}/T_{Re}. The ratio T_{Al}/T_{Re} can be written as $\exp -k^2(B_{Al} - B_{Re})$, so the uncertainty in the isotropic temperature factors gives an extra uncertainty in γ proportional to $Rk^2\sqrt{[(\Delta B_{Al})^2 + (\Delta b_{Re})^2]}$, where Δ represent the estimated standard deviation (ESD) in the following parameter.

Including all contributions,

$$\Delta(\mu_0 f(k)) = \sqrt{[\Delta\gamma(b_{Re} + b_{Al}R)]^2 + (\gamma \Delta b_{Re})^2 + \{b_{Al}Rk^2[(\Delta B_{Al})^2 + (\Delta B_{Al})^2]\}^2}. \qquad (7)$$

Equations (6) and (7) were used to obtain $\mu_0 f(k)$ and its ESD from the γ values using $\sqrt{(\Delta B_{Al}^2 + \Delta B_{Al}^2)} = 0.07$ Å^{-2} and $\Delta b_{Re} = 0.23$ fm. Except for a few high-angle reflections (k^2 large), the major contributor to the standard deviation is the ESD of the asymmetry itself.

Using the dipole approximation [Eq. (1)], $\mu_0 f(k)$ can be modeled using two parameters, a_{j0} and a_{j2}:

$$\mu_0 f(k) = a_{j0}\langle j_0(k)\rangle + a_{j2}\langle j_2(k)\rangle, \qquad (8)$$

where $\langle j_0(k)\rangle$ and $\langle j_2(k)\rangle$ are the values calculated by Blume *et al.* [20] for Sm^{3+}.

The $\mu_0 f(k)$ values obtained from the measured asymmetries were sorted in order of their measurement temperatures and divided into groups within which the temperature varied by no more than 1 K. For each group containing more than two reflections the values a_{j0} and a_{j2} and their estimated standard deviations were determined by a least-squares fit to Eq. (8). The values obtained are listed in Table II.

The dipole approximation equates the parameters a_{j0} and a_{j2} with the spin and orbital components of the magnetization and their sum to the ion's magnetization μ_0. Figure 3 illustrates the variation of these parameters between 30 and 100 K. Below 60 K both the spin- and orbital-aligned moments are about $2\mu_B$, with the orbital magnetization being slightly greater than the spin one. Between 60 and 65 K both fall rapidly and change sign at $T_{comp} \approx 66\,K$ (X1), $\approx 67\,K$ (X2), above which the aligned moments recover but with the orbital moment again slightly greater than the spin one. If M_L and M_S are the orbital and spin magnetic moments of the Sm^{3+} ion, for $T < T_{comp}$, $|M_L| > |M_S|$; at $T = T_{comp}$, $M_L = M_S = 0$, and for $T > T_{comp}$, $|M_L| > |M_S|$ again.

IV. DISCUSSION

Our results for the temperature variation of the spin and orbital moments of the Sm^{3+} ion in $Sm_{1-x}Gd_xAl_2$ $x = 0.024$ are very similar to those of Taylor *et al.* [15] for $x = 0.018$ measured by nonresonant x-ray diffraction, but the precision of the neutron results is much better ($\pm \approx 0.1\mu_B$) than that ($\pm \approx 0.8\mu_B$) for the x-ray data. Both sets of measurements suggest that the absolute value of the orbital magnetic moment of the Sm^{3+} ion is always greater than that of its spin moment except at T_{comp}, where both are zero. Although the differences determined at each temperature are hardly significant, their consistency in sign over the whole temperature range makes it highly likely that it is a real effect. Our results also agree with those of Taylor *et al.* [15] in indicating a reversal of both components with respect to the magnetizing field at T_{comp} which results in the ionic magnetization being opposed to the magnetizing field at temperatures above T_{comp}. This unexpected result was attributed by Taylor *et al.* [15] to a combination of unwanted beam movements from the synchrotron bending magnet and temperature fluctuations in the cryostat on reversing the applied field. However, neither of these fluctuations perturb the neutron measurements which are made with a stationary crystal under stable conditions of both temperature and field. In fact the reversal of the apparent magnetization with respect to the magnetizing field (neutron polarization direction) is a quite significant effect which can be seen even in the raw asymmetry data: the low-angle reflections of 220 and 113 have significant intensity asymmetries which

are positive at 30 K and negative at 100 K. It is, however, significant that both experiments showing the magnetization reversal derive the total moments μ_0 from diffraction data with $k > 0$. These do not include any contribution to the magnetization from conduction electrons for which the form factor is zero unless $k \approx 0$. The apparent magnetization reversal at T_{comp} is therefore probably due to the presence of magnetized conduction electrons ferromagnetically coupled to the rare-earth ion's spin moment. At low temperature the difference μ_0 between the orbital and spin components of Sm^{3+} is large, and the magnetization direction is that of the dominant orbital part. As the temperature is raised, μ_0 falls, and at T_{comp} it is exceeded by the magnetization of the conduction electrons. It is then the total spin moment, the sum of the ionic spin moment and that of the conduction electrons, which is aligned parallel to the magnetizing field. The ionic magnetization, still dominated by its orbital component, is therefore aligned in the reverse direction.

The observation that the reduction and reversal of both the spin and orbital components of the ionic magnetization takes place gradually over a range of about 10 K, rather than abruptly at T_{comp}, suggests that exact compensation occurs at different temperatures in different parts of the crystal, and this supposition is supported by the sharper transition observed in the smaller crystal. Since doping of $SmAl_2$ with Gd^{3+} ions is needed to achieve ZMF, it seems likely that the spin of the conduction electrons couples to the large spin moments of Gd^{3+} ions. The random positioning of the doping ions within the $SmAl_2$ lattice leads to a range in the conduction electron magnetization at the Sm sites and hence to the range in T_{comp}. Extrapolation of the absolute values of the spin and orbital moments across the transition region allows an estimation of their full values at T_{comp}. The resulting difference of $0.15(2)\mu_B$/Sm gives a value for the conduction electron polarization necessary to obtain the ZMF state at T_{comp}.

In conclusion the present investigation confirms that the compensation phenomenon in the ZMF compound $Sm_{1-x}Gd_xAl_2$ results from slightly different temperature dependencies of the spin and orbital moments of the Sm^{3+} ion. We have obtained accurate values for the variation of both the spin and orbital contributions to the magnetization of the Sm^{3+} ion in a field of 8T. These show that the spin component of the ionic magnetic moment never exceeds the orbital one, so that the ZMF state is not reached simply by equalization of the spin and orbital moments of Sm^{3+} ions. It is already known that doping of $SmAl_2$ with Gd is necessary to achieve the ZMF state. The gradual reversal of both the spin and orbital moments of Sm^{3+} ions over a range of $\approx 10\,K$ around T_{comp} suggests that compensation is achieved by enhancement of the conduction electron polarization by the randomly substituted Gd^{3+} doping ions.

[1] J. H. Van Vleck, *The Theory of Electric and Magnetic Susceptibilities* (Oxford University Press, Oxford, 1932).

[2] H. J. Zeiger and G. W. Pratt, *Magnetic Interactions in Solids* (Clarendon, Oxford, 1973).

[3] K. W. H. Stevens, *Magnetic Ions in Crystals* (Princeton University Press, Princeton, NJ, 1997).

[4] M. Z. Hasan and C. L. Kane, Rev. Mod. Phys. **82**, 3045 (2010).

[5] C. L. Kane and E. J. Mele, Phys. Rev. Lett. **95**, 146802 (2005).

[6] C. L. Kane and E. J. Mele, Phys. Rev. Lett. **95**, 226801 (2005).

[7] C. Wan, Y. Wang, N. Wang, W. Norimatsu, M. Kusunoki, and K. Koumoto, Sci. Technol. Adv. Mater. **11**, 044306 (2010).

[8] A. I. Boukai, Y. Bunimovich, J. Tahir-Kheli, J. K. Yu, W. A. Goddard, III, and J. R. Heath, Nature (London) **451**, 168 (2008).

[9] H. Ohta, S. Kim, Y. Mune, T. Mizoguchi, K. Nomura, S. Ohta, T. Nomura, Y. Nakanishi, M. Hirano, H. Hosono, and K. Koumoto, Nat. Mater. **6**, 123 (2007).

[10] J. P. Heremans, V. Jovovic, E. S. Toberer, A. Saramat, K. Kurosaki, A. Charoenphakades, S. Amanaka, and G. J. Snyder, Science **321**, 554 (2008).

[11] L.-D. S.-H. Lo, Y. Zhang, H. Sun, G. Tan, C. Uher, C. Wolverton, V. P. David, and G. Kanatzidis, Nature (London) **508**, 373 (2014).

[12] E. A. Turov, *Physical Properties of Magnetically Ordered Crystals* (Academic, New York, 1965).

[13] H. Adachi and H. Ino, Nature (London) **401**, 148 (1999).

[14] H. Adachi, H. Kawata, H. Hashimoto, Y. Sato, I. Matsumoto, and Y. Tanaka, Phys. Rev. Lett. **87**, 127202 (2001).

[15] J. W. Taylor, J. A. Duffy, A. M. Bebb, M. R. Lees, L. Bouchenoire, S. D. Brown, and M. J. Cooper, Phys. Rev. B **66**, 161319(R) (2002).

[16] S. Qiao, A. Kimura, H. Adachi, K. Iori, K. Miyamoto, T. Xie, H. Namatame, M. Taniguchi, A. Tanaka, T. Muro, S. Imada, and S. Suga, Phys. Rev. B **70**, 134418 (2004).

[17] F. L. Pratt, S. J. Blundell, T. Lancaster, M. L. Brooks, C. A. Steer, and H. Adachi, Physica B (Amsterdam, Neth.) **374–375**, 34 (2006).

[18] H. J. Gotsis and I. I. Mazin, Phys. Rev. B **68**, 224427 (2003).

[19] W. Marshall and S. W. Lovesey, *Theory of Thermal Neutron Scattering* (Oxford University Press, Oxford, 1971), Chap. 5, p. 109.

[20] M. Blume, A. J. Freeman, and R. E. Watson, J. Chem. Phys. **37**, 1245 (1962).

[21] J. E. Lynn and P. A. Seeger, At. Data Nucl. Data Tables **44**, 19 (1990).